Review

Advances in Electronics Prompt a Fresh Look at Continuous Wave (CW) Nuclear Magnetic Resonance (NMR)

Michael I. Newton, Edward A. Breeds and Robert H. Morris *

School of Science and Technology, Nottingham Trent University, Nottingham NG11 8NS, UK;
michael.newton@ntu.ac.uk (M.I.N.); edward.breeds@ntu.ac.uk (E.A.B.)

* Correspondence: rob.morris@ntu.ac.uk; Tel.: +44-115-848-3123

Abstract: Continuous Wave Nuclear Magnetic Resonance (CW-NMR) was a popular method for sample interrogation at the birth of magnetic resonance but has since been overlooked by most in favor of the now more popular pulsed techniques. CW-NMR requires relatively simple electronics although, for most designs, the execution is critical to the successful implementation and sensitivity of the system. For decades there have been reports in the literature from academic groups showing the potential of magnetic resonance relaxation time measurements in industrial applications such as the production of food and drink. However, the cost, complexity and power consumption of pulsed techniques have largely consigned these to the literature. Advances in electronics and developments in permanent magnet technology now require a fresh look at CW-NMR to see if it is capable of providing cost effective industrial solutions. In this article, we review the electronics that are needed to undertake a continuous wave NMR experiment starting with early designs and journeying through the literature to understand the basic designs and limitations. We then review the more recent developments in this area and present an outlook for future work in the hope that more of the scientific community will take a fresh look at CW-NMR as a viable and powerful low-cost measurement technique.

Keywords: continuous wave nuclear magnetic resonance; CW-NMR; spectrometer

1. Basic Principles of Continuous Wave Nuclear Magnetic Resonance

Nuclear magnetic resonance (NMR) is an extremely powerful tool, capable of non-invasively providing information about molecular environments and their fundamental physical properties. Since the birth of the nuclear magnetic resonance experiment in the 1930s [1,2], significant advances in understanding and utilizing the technique [3–5], alongside an ever increasing number of applications [6–9], have led NMR to the forefront of analytical techniques used in physics, chemistry and medicine. Two of the most notable contemporary applications of magnetic resonance are Magnetic Resonance Imaging (MRI) and Chemical Shift NMR Spectroscopy (often referred to simply as NMR).

NMR uses the response of the intrinsic nuclear magnetic moment of certain nuclei to externally applied magnetic fields and the application of appropriate Radio Frequency (RF) signals to probe their local environment.

Nowadays, more common is the so called Pulsed NMR experiment—these nuclear magnetic moments can, from a classical mechanics perspective, be considered as microscopic bar magnets that align themselves with a strong applied magnetic field (along an arbitrary z-axis). RF radiation at a frequency ω is then applied, to satisfy the so-called Larmor condition [10] (see Equation (1)), which

tips these magnetic moments such that they are normal to the original field (and the spins lie in the x-y plane).

$$\omega = \gamma B_0 \tag{1}$$

In this expression, ω is the frequency of precession of a given nuclei within a magnetic field of magnitude B_0. The gyromagnetic ratio γ is a constant of proportionality characteristic of the nuclei (42.58 MHz T^{-1} for the proton). The principle of reciprocity suggests that applying energy at this same frequency will yield optimum manipulation of the magnetic moments. For most pulsed experiments utilizing protons, this is in the radio frequency range and so this is often termed an RF pulse. The tipped moments then rotate in the x-y plane (a motion termed precession) about the axis of the external magnetic field at a rate dependent on their local field strength. The net magnetization vector has sufficient magnitude that electromagnetic induction in a coil surrounding them, after amplification, yields a detectable signal. Within this signal are components for each frequency of precession and hence information about the local magnetic fields. In Chemical Shift Spectroscopy, these frequencies provide molecular information, in MRI they encode spatial information. Both of these experiments are grouped under the wider title of Fourier transform magnetic resonance (FT-MR). A large number of commercial low-cost pulsed NMR systems are available, although for many applications these are still considerably more expensive than is viable for many sensor applications. In recent years, a number of ultra-low-cost systems have been discussed in the literature but, to date, none have reached the stage of development which allows them to be commercially deployed.

Continuous wave magnetic resonance on the other hand, more commonly called Continuous Wave Nuclear Magnetic Resonance (CW-NMR), has largely been neglected for the past half century. Despite being the forerunner of the pulsed experiment, the technology of the time provided a comparatively poor signal, requiring significant effort in set up and tuning, ultimately leading to the demise of CW-NMR for all but a small handful of applications. In contrast to the FT-MR experiment, the CW-NMR experiment is simpler: sweeping the sample through the Larmor condition with a time varying magnetic field or frequency of irradiation, while monitoring the amount of energy which it absorbs. Investigating the absorption of the RF energy by the ensemble of magnetic moments provides information about their quantity and environment [11].

CW-NMR is today found in many undergraduate physics laboratories and is seen by many as a useful teaching aid in understanding magnetic resonance, given its comparative simplicity. Almost all such experiments however still employ oscilloscope detection, despite the prevalence of fast data capture hardware, capable of digitizing even the raw RF signals with minimal cost. In this article, we present a review of the wide array of electronic hardware that has been used to undertake the continuous wave NMR experiment throughout the existence of the technique, followed by a discussion on the quantification of material properties. The final section considers how modern electronics are allowing the more basic of the NMR techniques to be used in a quantitative sense, in the hope that more scientists will consider CW-NMR for low-cost automated measurements of material properties.

2. Humble Beginnings

Although the first successful magnetic resonance absorption experiments reported by Purcell, Torry and Pound in 1946 [3] utilized a bridge circuit, which will be discussed in the next section; the most basic CW-NMR experiment was reported in 1949 by Rollins [12] and is shown in Figure 1. A signal generator is used to supply RF to a tuned circuit through a resistor, resulting in a constant current signal, and the magnetic field in which the sample sits is varied using so-called sweep coils. During this process, the amplitude of the RF is monitored (after it is amplified and rectified). As the field of the sample approaches resonance, more energy is absorbed and hence the amplitude of the RF signal becomes ever lower until the Larmor condition is met. The signal then increases back to equilibrium as the field continues to change.
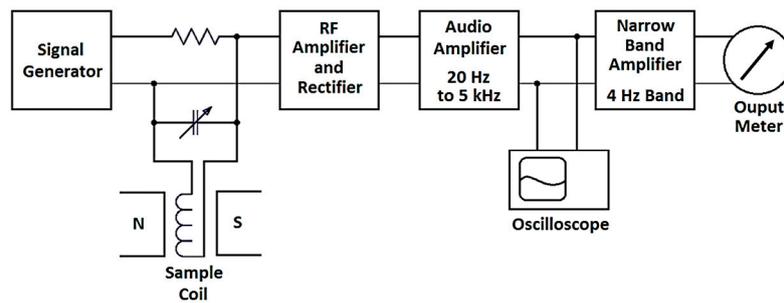
Figure 1. Rollins basic Continuous Wave Nuclear Magnetic Resonanceexperiment.

The limiting factor in this, and any such system, relates to the order of magnitude of the amplitude modulation due to absorption. This was calculated for protons in water at 21.3 MHz by Andrew [13] to be less than 1%, which represents the best-case scenario. This means that significant amplification is required and, for improved signal to noise ratio, the original class of circuit utilizing bridges is in fact preferable. In such a setup, only the change in signal due to the absorption is amplified, providing a far higher dynamic range than in any amplifier setup. Examples of bridge circuits are discussed in the following section.

3. Bridge Circuits

As alluded to in the previous section, a popular means of monitoring RF absorption is the use of a bridge. This circuit design utilizes at least two so-called arms, which, in the absence of a sample, have similar impedance. When a sample is introduced, the relative impedance changes at the frequency of absorption and a voltage appears at the output of the bridge. As a result, when off resonance, the amplifier only needs to amplify noise, not a maximal signal as in the example of Figure 1, and hence one can use far more sensitive electronics. Off resonance, the output of the bridge is noise rather than signal. When the magnetic field is then swept through resonance, a voltage becomes present at the output, which is fed to a sensitive preamplifier. Such circuits are also very popular in magnetometers where the resonance of a known sample is used to determine the magnetic field in which the sample sits [14], with a schematic for such a circuit shown in Figure 2. It should be noted that it is essential to undertake careful balancing of any bridge circuit [15]. That is to say that if the two arms of the bridge, off resonance, are not sufficiently similar in terms of their impedance, the output will be RF leakage which may be sufficient to overload a sensitive detector.
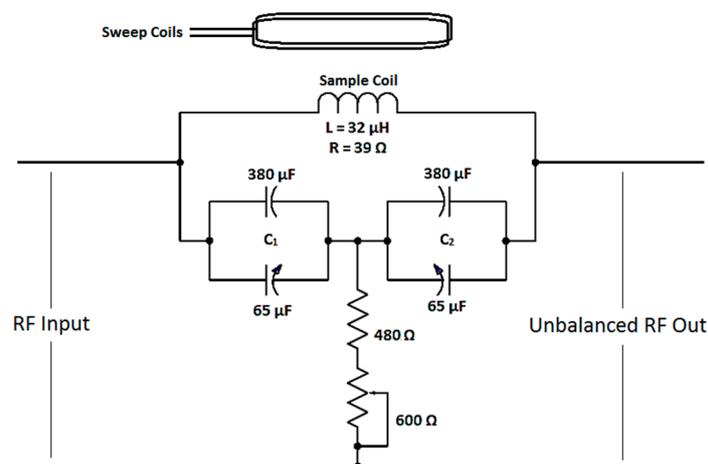
Figure 2. An example bridge circuit used in an early magnetometer to determine magnetic field strength.

In most cases, bridge balancing is a complex and time-consuming process that requires significant skill and patience on the part of the experimentalist. A possible solution to this was suggested in 1957, where voltage controlled capacitors were employed to allow for automatic bridge balancing [16]. A small oscillating voltage with high frequency is used to check for balance, which is then automatically corrected with minimal deterioration of the NMR signal (see Figure 3). This represents an elegant solution to the issue of balance which has not been widely adopted, despite the ease of operation.
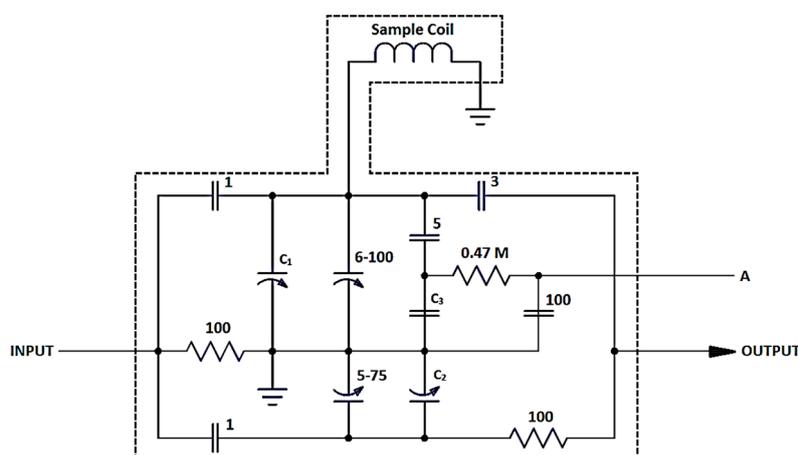
Figure 3. An example of automatic bridge circuit balancing (Correction voltage applied through A).

The output signal from a bridge circuit is however very small and often buried within the noise floor. To combat this, a rectifier and lock-in amplifier are employed, the fundamental principles of which will be discussed here, with the reader referred to an excellent description for further detail [17]. For very weak signals that vary with a well-known periodicity, and for which the bandwidth of traditional amplifiers would lead to signal to noise ratios less than 1, lock-in amplification allows for accurate extraction. Lock-in amplifiers are based around the principles of a phase based detector, which utilizes a reference signal with similar frequency to (or sometimes twice that of) the signal of interest. The output of the phase sensitive detector is the sum and difference of the two input signals. By filtering out the sum component with a low pass filter, only the difference is output, which, for cases of the same frequency input and reference, leads to a DC voltage proportional to the input voltage. This voltage is then fed to a traditional amplifier which now only has the variations of interest to amplify and hence can do so with a far greater SNR output. In works such as Bloembergen and other utilizing bridges, the modulation coil voltage is used as the lock-in reference [18], although this can also be achieved by applying an additional audio frequency to the sweep, which offers further sensitivity to the reference.

4. Double Coil Circuits

In the systems discussed thus far, the amount of energy absorbed by the sample has been determined by measuring the absence or imbalance of an RF signal on resonance. A less frequently used setup, sees the use of two coils, one of which delivers RF energy to the sample in one direction while the other subsequently measures the resulting signal from precession in an orthogonal direction. With accurate alignment, the incident RF can be eliminated from the receive electronics chain, allowing for very sensitive preamplifiers and minimal noise [11,19]. The challenge with such a setup, as with balancing the bridges of the previous experiments, is the requirement of ensuring that there is minimal leakage from the first coil into the second. The typical method of achieving such a condition is to utilize a metallized paddle [11], as shown in Figure 4, to steer the flux lines of the transmit solenoid to one side or the other, thus allowing almost complete isolation of the two coils (second coil not shown).
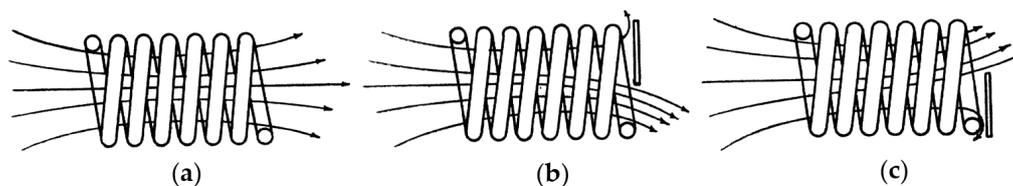
Figure 4. Flux steering method. (reproduced with permission from [11]. Copyright American Physical Society, 1946) (**a**) Unperturbed magnetic flux generated by a solenoid; a metallized paddle being used to steer flux (**b**) downwards or (**c**) upwards in the same coil. The receive coil is not shown.

In some laboratory experiments, such as that shown in Figure 5, this is further aided by the use of a waveguide and physical separation of the coils by some distance [20].
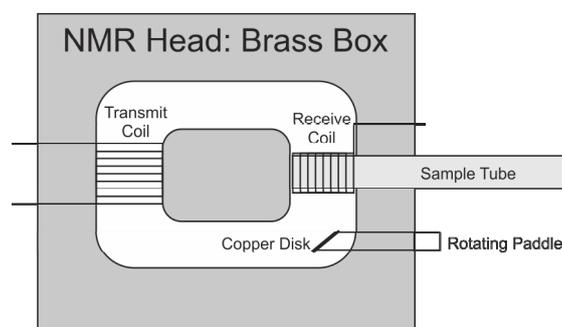
Figure 5. Further coil isolation using a waveguide and physical separation.

Although the so-called transmit and receive chains (referring to the path leading to the first coil delivering the RF and that leading away from the second coil detecting the NMR signal, respectively) are normally isolated from each other, a bridge may be introduced between the two coils [19] which can be used to suppress any leakage. This may further improve the signal to noise ratio.

5. Non-Isolated Oscillator Circuits

Thus far, our discussion has been limited to RF sources that are essentially isolated from the resonant portions of the circuits. That is to say, as the sample is swept through resonance, the RF source remains unchanged. In the next sections we will consider a class of circuit where the RF source is in fact resonant with the sample and varies in some way as the sample is swept through resonance. This allows us to move away from the stringent requirements for balancing bridges. Oscillator driven systems are more convenient in many applications, particularly magnetometers where it is only the amplitude of the absorption signal and not its shape or width (known as the linewidth) that is important. We will first consider circuits utilizing a magnetic field sweep, which we have primarily looked at so far, followed by circuits for which the field remains unchanged whilst the frequency is swept.

5.1. Oscillator Circuits Using Magnetic Field Sweep

In this section we will review two types of oscillators which are used when the magnetic field of the sample is swept whilst being driven by an oscillation at a continuous frequency. The first class of such an oscillator is known as the marginal oscillator.

5.1.1. Marginal Oscillators

One of the most frequently employed oscillator type circuits for use in continuous wave NMR is the marginal oscillator. The basis of this system is a tank circuit comprising a sample coil and

a capacitor. This is then driven with energy from a valve or transistor circuit which is just sufficient to sustain oscillation. Any subsequent increase in loading, as caused by sweeping through resonance, results in a reduction in amplitude which can be subsequently detected with methods such as those that we have already considered.

　　Figure 6 shows a possible signal obtained during a sweep of the magnetic field, showing amplitude modulation caused by the change in loading. It should be noted that in this example, the RF energy is of a significantly lower frequency than would be expected in a real experiment and the depth of the dip is significantly larger. As a result, diode detection is normally required and is found in almost all receiver circuits. After it is rectified, the signal is normally passed through an audio frequency or lock-in amplifier.

Figure 6. An example of amplitude modulation caused by changes in loading. Note that the width of the dip is greatly exaggerated for clarity.

　　Unlike the bridge circuits, where a change in the resonance condition must be accounted for by retuning the RF source, the marginal oscillator is itself part of the resonant circuit and thus tracks the resonance. This leads to the significant advantage that the detected signal is purely absorption, thanks to the inherent feedback. Any dispersive component of susceptibility produces slight frequency modulation of the oscillator, which is not rectified in the detection stage. The classic paper describing the bench mark valve based marginal oscillator is by Pound and Knight [21], shown in Figure 7.

Figure 7. The classic valve based marginal oscillator. (reproduced with permission from [21]. Copyright AIP, 1950).

Some ten years later, with the increasing availability of transistorized electronics, Donnally and Saunders [22] published a greatly simplified version based around a 2N393 PNP Germanium transistor. Although the SNR is about half that of the Pound circuit shown in Figure 7, it exhibits very low power consumption and does not suffer from the problems of microphonics (conversion of mechanical movement to noise) presented by the valve circuits. In Figure 8, the Donnally and Saunders marginal oscillator is shown, based on a tank circuit feeding into the base of the Germanium transistor, the output of which passes through a diode rectifier and narrow bandwidth audio filter with a cut off at twice the sweep rate of the magnetic field modulation coils. The paper also provides an audio amplifier circuit which is of standard design. Although the presented work is based upon swept magnetic fields, the authors state that C_1 and C_2 can be substituted with voltage variable capacitors to allow for a variable oscillator sweep.
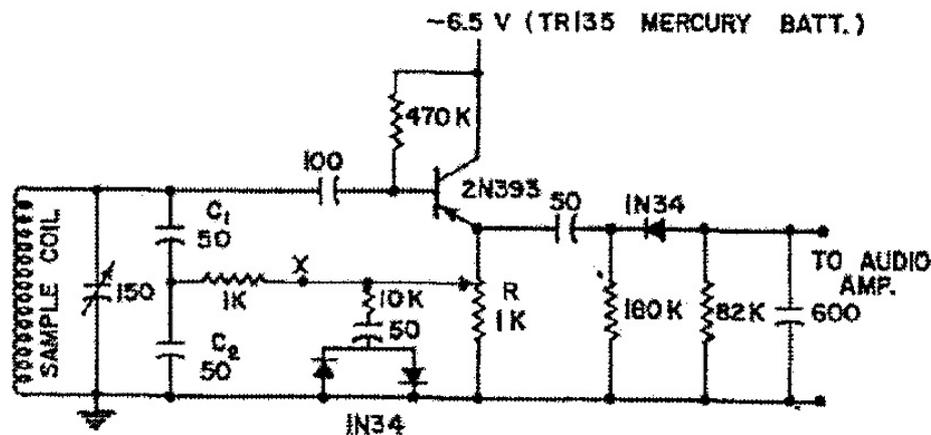
Figure 8. The Donnally Saunders marginal oscillator. (reproduced with permission from [22]. Copyright AIP, 1960).

The early circuits operated successfully thanks to a number of transistor parameters that are undesirable for many modern designs (such as those that limit maximum frequency of operation in amplifier circuits). As transistor technology has continued to improve, the availability of suitable transistors became challenging. In a thesis by Frank Willingham [23], this issue was addressed by replacing the Germanium transistor of the Donnally Sanders circuit with a pair of Field Effect Transistors (FETs). As well as substituting components for what were then state of the art, the circuit was also upgraded for an improved source following the replacement of the traditional resistor with a second FET. This provides greatly enhanced source following and enhanced impedance matching, which is of great benefit in a circuit where load mismatch is largely responsible for the detected signal. An Operational Amplifier based audio amplifier is also presented, which is of standard design. Lock-in detection is also used in this work, with one sweep coil used for sweeping the resonance of the sample, whilst a second applies a small, higher frequency oscillation, which is fed to the phase sensitive detector.

5.1.2. Non-Marginal Oscillators

Around the same time that Donnally and Sanders were updating the Pound circuit, Robinson published a paper [24] describing the disadvantages of marginal oscillators. He suggests that there are three drawbacks:

> "Firstly, they are less sensitive; secondly, they are difficult to adjust at levels below about 20 mV; and finally they cannot be used with circuits of a low inductance to capacitance ratio. If the shunt impedance of the tuned circuit is low, not only is the noise figure impaired but also the circuit may fail to oscillate at all."

He provided an alternative which has become known as the Robinson oscillator [24]. The primary difference between a marginal oscillator and a Robinson oscillator is the feedback loop. Instead of directly feeding back the signal through a resistor, it is fed back through a limiter thus returning a square wave current back to the tank circuit. The construction of a tank circuit is such that it will act as a filter to select the fundamental of the square wave as shown schematically in Figure 9. This ensures that the only non-linearity of the circuit occurs in the limiter, allowing for better prediction and control of the overall oscillation. In other words, the Robinson oscillator is a non-marginal oscillator.
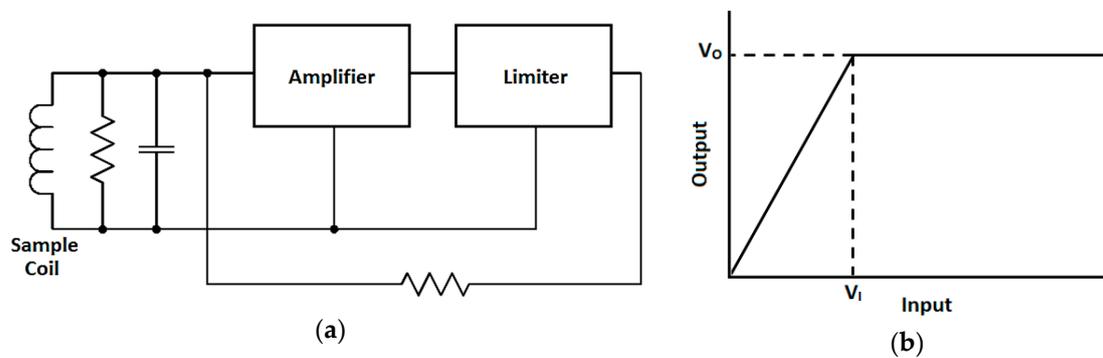
Figure 9. (**a**) Limited self-oscillator; (**b**) Ideal characteristics of the limiter.

Although the original design [25] utilized valves, an updated transistorized version was published in 1965 [26].

Faulkner and Holman however, in a publication two years later [27], claimed that a large number of transistorized Robinson oscillators that had previously been published were in fact not true to the functionality of the original. They found, in fact, that even that published by Robinson himself in the 1965 paper did not meet the original feedback criteria. Following discussions with Robinson, Faulkner and Holman produced a transistor version of a true Robinson oscillator, shown in Figure 10. By way of demonstration, they used their circuit as a magnetometer with a rubber sample material up to a frequency of 30 MHz.

Figure 10. A true transistorized Robinson oscillator.

An alternative strategy to the use of discrete transistors was described by Deschamps, Vaissiére and Sullivan [28], utilizing the CA3102 chip that has two independent differential amplifiers (although only the second is used differentially here) with associated constant current transistors on a common monolithic substrate. This arrangement (shown in Figure 11) allows for increased bandwidth and input impedance, giving greater stability of measurement and a significant increase in gain whilst utilizing a single integrated circuit.

Figure 11. Non-marginal oscillation utilizing the CA3102 chip. (reproduced with permission from [28]. Copyright AIP, 1977).

Some years later, in 1990, a MOSFET version of a true Robinson oscillator was reported by Wilson and Vallabhan [29]. The use of MOSFETs allows for significant reduction in Q-factor loading of the tank circuit, giving a higher dynamic range for the NMR signal since the shunt impedance of the tank circuit is significantly lower than the input impedance of the MOSFET. They also reduce $1/f$ noise and, thanks to their good transconductance, can be operated at much lower RF levels.

5.2. Oscillator Circuits Using Frequency Sweep

The second type of oscillator, where the magnetic field is constant whilst the sample is driven through resonance by changing the RF frequency, is used extensively for magnetometer applications. This allows for smaller devices (as there are no sweep coils required) and exploration of a greater range of fields than can be achieved by retuning field sweep oscillators. In a 1951 paper by Knoebel [30], a transitron oscillator is used [31] that utilizes a minimal number of components (see Figure 12) to generate oscillations. The oscillation frequency of such a circuit can be controlled by a single capacitor, allowing for simple tuning of such a device although the final circuit deployed to facilitate the measurement of the resonant frequency of the sample is significantly more complicated.

Figure 12. A simple frequency sweep magnetometer.

The final circuit of the Knoebel and Hahn work was modified to utilize transistors in 1966 [32]. In addition to the replacement of the valve elements, a remote tuning capacitance is added as an electrically tuned varicap diode (CR1 in Figure 13), allowing for an automated sweep of the frequency equivalent to the field sweep in the alternative class of oscillator.
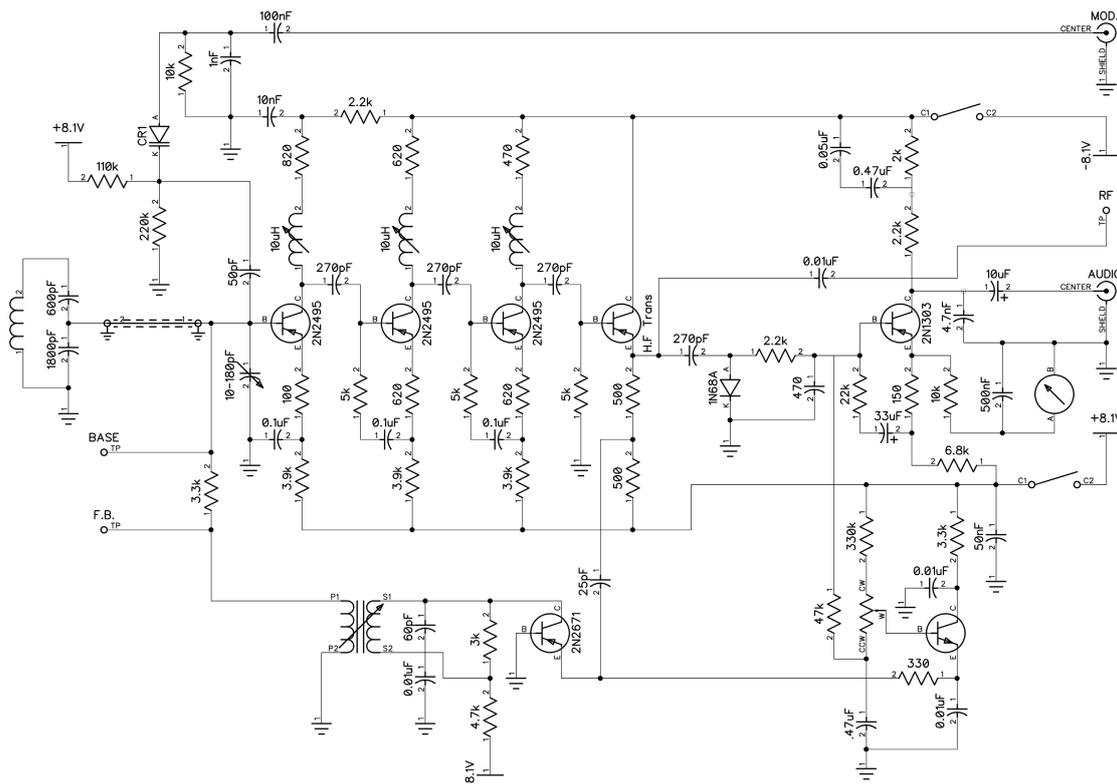
Figure 13. A frequency sweep oscillator utilizing transistors.

Varicap diodes are however challenging to work with and do not allow for as wide a tuning range as desired for maximum convenience. They are however also used in the more recent Robinson work [33] for a magnetometer.

The same concept can be found for a low field magnetometer presented by Weyand [34], which is shown in Figure 14, where a pair of back to back varicap diodes are substituted for the original tuning

capacitors on the tank circuit allowing for a greater range of tuning and also for accurate tuning at field below 50 mT, which are typically challenging to measure.
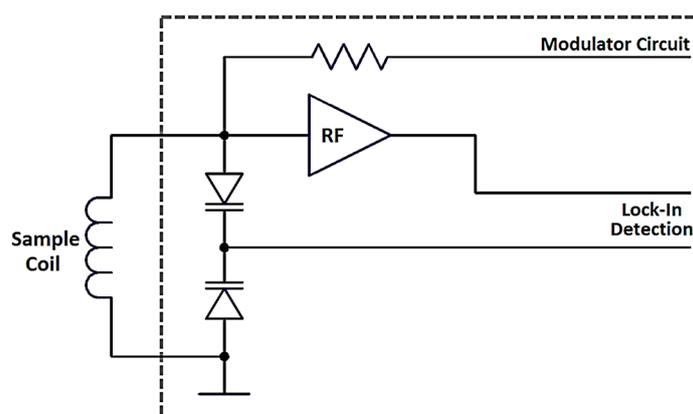
Figure 14. Front end of Weyand's low field magnetometer, utilizing varicap diode tuning.

Such designs continue to enjoy commercial success as magnetometers (e.g., Metrolabs precision teslameter PT2025 [35]).

An alternative circuit design known as a Q-meter have been used increasingly in low temperature experiments to investigate processes such as chemical group rotation since the 1980s [36]. Such circuits use similar detection processes where the absorption or dispersion signals, or both, are recorded at a range of frequencies [37] with double lock in detection to sweep the tuning of the circuit with the applied RF, thus measuring the circuit Quality, Q. By changing the phase of the lock-in amplifier employed in such a configuration, the dispersion and absorption can be simultaneously recorded.

In addition to low temperature experiments, Q-meters have also been used more recently for nuclear and particle physics experiments where similar devices are used to measure the polarisation of metallic targets held at low temperatures in magnetic fields [38]. In more recent years, developments have been made to improve the noise levels of such devices particularly for non-proton signals and those which result from polarisation driven by Dynamic Nuclear Polarisation (DNP) [39]. In such experiments, the sample is irradiated with microwaves, which results in electron excitation. The energy of the excited electrons is then transferred to the nuclei of interest by various processes. CW-NMR provides a highly sensitive method of detection of the level of polarisation that is affected by nuclear irradiation thus allowing indirect detection of changes to the sample.

6. Relaxation Measurements with CW-NMR

Although rarely performed given the prevalence of pulsed magnetic resonance, it is possible to measure both the spin-lattice relaxation time T_1 (the time constant of the loss of energy to the surrounding lattice) and the spin-spin relaxation time T2* (not actually a loss of energy, but the time constant of the loss of phase between neighboring nuclei) of a sample, both of which provide characteristic information. In the coming subsections, we will review strategies for measuring these time constants and their applications.

6.1. Measuring the Spin-Lattice Relaxation Time Constant

The return of the excited nuclei to their equilibrium state occurs with a time constant T_1, the measurement of which is notoriously time consuming with pulsed magnetic resonance. Several ingenious methods of measuring this value with continuous wave magnetic resonance have been published in the literature.

One of the first experiments measuring T_1 was published in 1949 by Drain [40] and is an extension of the original work by Bloch [11]. The principle of detection is that with two crossed coils, one used

to excite the sample and one to detect the resulting absorption, the time at which the absorption is measured dictates the polarity of the signal. During the course of a sweep cycle, the magnetisation tends towards equilibrium exponentially. Where the sweep rate is on the same order as the T_1 time, this change will be happening whilst the system is above and below resonance. When the sweep voltage is balanced about resonance, the peak generated sweeping from low to high will have the same amplitude as the peak sweeping back. If the sweep voltage is offset above or below resonance however, the two peaks will have different amplitudes. Plotting the amplitude of either of these peaks as a function of the difference between the time spent above and below resonance results in a trace of the T_1 relaxation. The author goes on to verify this with measurements of the T_1 value for glycerine protons at different temperatures and hence viscosities.

An alternative strategy, such as that used in the work of [13] is to drive the sample with a very low RF signal such that it takes several sweeps through resonance to cause saturation of the nuclei of interest. In this experiment, each absorption trace is collected and plotted as a function of the integral of the applied RF. The amplitude of the absorption traces will change exponentially with T_1. This method, although relatively accurate, requires an exact measurement of the RF field.

In a strategy more akin to pulsed NMR's inversion recovery experiment, the sample is saturated on resonance and quickly swept off resonance for a time and then swept back through resonance [13]. The amplitude is plotted against the time between sweeps which again yields an exponential with time constant T_1. This is an excellent method for easily saturated samples with very long T_1 values, ideally well over 5 s. A similar method, presented in 1983 by Firth [41], uses a commercial Newport magnetometer based on a Robinson oscillator. Before the start of the experiment, the sample is saturated either with significant RF power or low modulation amplitude. The saturation is then suddenly reduced (either by reducing the RF power or increasing the modulation amplitude). The signal recovers with a time constant ZT_1, where $Z = (1 + 2PT_1) - 1$ and P is the probability of inducing a nuclear transition for the nuclei of interest (which should technically be a function of the RF intensity and field magnitude, which is not included here as it was not in the original work). Such a recovery was recorded with an oscilloscope camera by way of demonstration, which is shown in Figure 15.
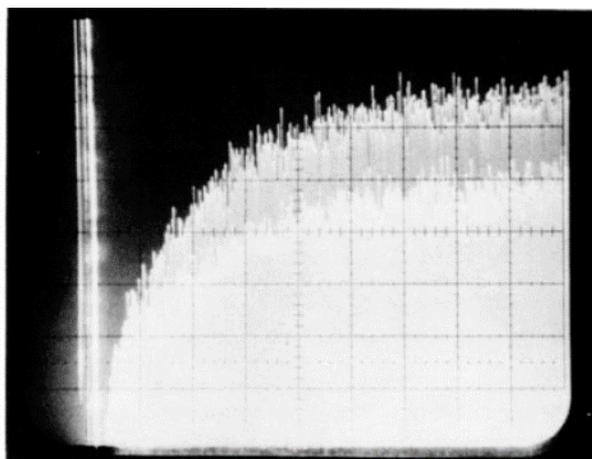
Figure 15. Oscilloscope trace of the proton recovery of water. (reproduced with permission from [41]. Copyright IOP, 1982).

An elegant measurement of T_1 was presented by Donnally in 1963 [42], where different flow rates of the sample down a pipe are used to vary the amount of time that the sample spends in the presence of the field. The sample passes through a coil connected to the marginal oscillator described in their earlier paper [23], a schematic for which can be seen in Figure 16. The nuclear spins of the sample are unaligned while outside of the magnetic field and become polarized as they enter (exponentially with time constant T_1). For very rapid flow rates, the sample has had little time to become polarized and

hence will have a small signal and as the flow rate becomes smaller the signal increases up to the time at which the sample is fully polarized, after which decreases in flow rates will not increase the signal amplitude. By plotting the signal amplitude against the time from the edge to the center of the magnet, an exponential with time constant T_1 is traced. Using this method, the authors measure T_1 down to 0.2 s.
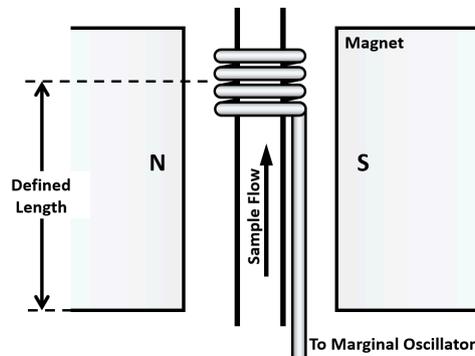
Figure 16. The experimental arrangement, described by Donnally, for measuring T_1 using a varied flow.

An alternative method proposed in 1968 by Look and Locker [43] utilized a gated sweep waveform. In this method, the sample is left aligned with the magnetic field, which is held off resonance before the start of the measurement. A number of cycles of the sweep coils follow during which each absorption trace is collected. The amplitudes of each trace vary exponentially with time constant T_1 (see some example traces in Figure 17) until saturation is reached. Such a method was relatively easy to automate even in the late 60s, although automatic processing was not available.
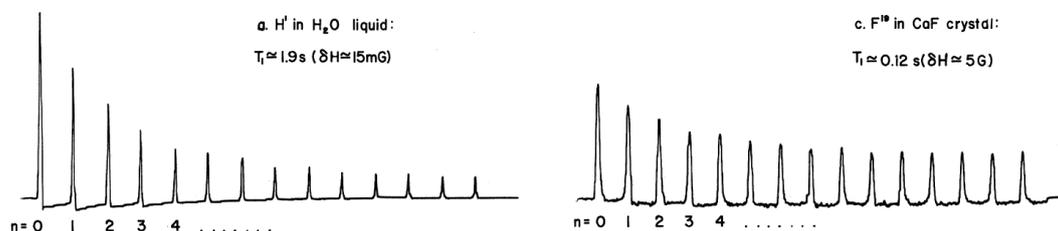
Figure 17. Example traces from the Look and Locker experiment. Each peak is an individual absorption signal collected after n full cycles of the sweep signal showing an exponential reduction in signal amplitude. The left figure is the signal from protons in water, the right figure is the signal from Fluorine in Calcium Fluoride. (reproduced with permission from [43]. Copyright American Physical Society, 1968).

6.2. Measuring the Spin-Spin Relaxation Time Constant

In a pulsed experiment, the direction of some of the nuclei of interest are aligned and allowed to precess. As they do so, they generate a miniscule field that perturbs their neighbors, leading to fractionally different precessional frequencies. Over time (from microseconds to a few seconds in most samples), the number of nuclei rotating through the original point every revolution decreases exponentially. Where this can be measured, the time constant is known as T2* in a continuous wave system, energy is supplied off resonance, which has little if no effect on the nuclei of interest. At the point at which we approach resonance, we begin to affect the nuclei. As we then sweep past resonance, the signal may continue to exist thanks to this T2* storage of energy. For samples with long T2*, this will have a more significant effect than for those with short T2*. As such, assuming that the sweep of field or frequency is sufficiently slow to approximate the steady state absorption, T2* can be determined from the line width of the absorption signal. $R_2 = (1/T2^*)$ is proportional to the half-height

width of the absorption peak or the interval between the maximum and minimum slope. A particularly nice treatment of the numerical form for both Gaussian and Lorentz absorption line shapes is provided by Andrew [13]. Such measurements have been used for wide ranging applications such as Iron concentration measurements and glycerin viscosity and temperature variation [39].

An alternative method for determining T2* is presented by Bloembergen et al. [19], utilizing a beat signal termed wiggles. This beat signal is caused by the increasing difference between the frequency of the nuclei that are still precessing, which increases as the field sweep continues, and the RF excitation frequency. This leads to a signal (grey in Figure 18) which decreases exponentially with T2* and which becomes increasingly higher in frequency as a function of the sweep rate [44].
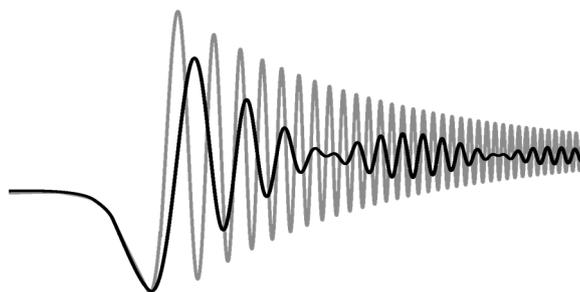
Figure 18. Beating caused by differences in the frequency of rotation of precessing nuclei and RF excitation.

Such a signal will be seen where the sweep rate does not approximate the steady state, i.e., is short compared with $1/\gamma\Delta H_0$, where ΔH_0 is the inhomogeneity in the field. Useful guidance is provided [45], suggesting that the sweep must be at least ten times faster than the shortest T2* value of interest to achieve such a signal. In the literature, this experiment is often referred to as the fast passage experiment.

As the inhomogeneity of the field increases, the distribution of precessional frequencies causes an additional beat frequency such as that seen in the Black curve of Figure 18, which are reviewed in the publication of Gabillard [46]. As the inhomogeneity continues to increase, it becomes progressively more difficult to meet the criteria for fast passage and it ultimately becomes impossible to measure T2* using such a method.

There are remarkably few reports past the 1960s of CW-NMR being used for T2* measurements. Given the prevalence of monitoring T2* with pulsed NMR for industrial applications, one would expect that a technique that would allow T2* to be measured for a small fraction of the cost of a commercial pulsed system would be commonplace, but this is not the case. Even CW-NMR teaching instruments avoid the measurement of T2* in their guidance literature. The stringent requirements for high field homogeneity (required to satisfy the condition by which the sweep rate is short compared to $1/\gamma\Delta H_0$) are most likely the reason for this, combined with the difficulty of determining the value of T2* which is straightforward with pulsed NMR.

6.3. Amplitude Measurements

Although high resolution FT-NMR offers qualitative answers to complex, structure oriented problems in chemistry and physics, amplitude measurements of CW-NMR offer a solution that is both easier to implement and interpret for high throughput, quantitative analysis.

As well as offering a simple nucleus-counting tool (where the amplitude of a signal is proportional to the number of contributing, precessing magnetic moments), atoms of a solid have a restricted motion compared to those of a liquid. This restriction is reflected in the resonance profile of the magnetic moments, with a broad resonance associated with solids, and a narrow peak with liquids, with

integrals proportional to the number of nuclei. This difference in line-shape then allows isolation of the individual components of the signal using suitable filters and adjustment of the NMR instrumentation.

The ability to differentiate between states of matter, particularly bound and unbound water, prompted many agricultural, industrial and food based applications in CW-NMR. Early examples of this looked at signal amplitude to evaluate the water content of foodstuffs such as apple and potato [47]. An interesting example [48] also presented an experiment where the proton signal in coal is first determined before the sample is wetted. After the ingress of water, an additional sharper resonance is seen effectively overlaid atop the original coal signal (see Figure 19).
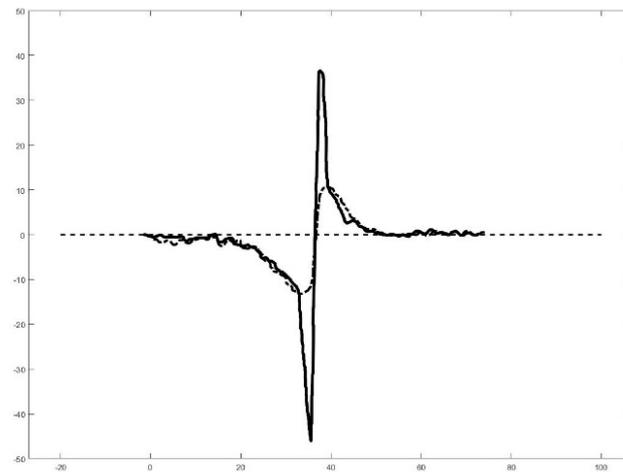
Figure 19. Dashed line is absorption signal from dry coal as a result of naturally present protons. The solid line follows the ingress of water. Notice the shoulder on the solid line as a result of the original protons.

This was followed by investigations of liquid-to-solid ratio, initially in chocolate [49], using the amplitude of the wide-line peak associated with the hydrogen signal of fat. This wide-line method was also compared to traditional ways of measuring fat content at the time, such as dilatometry (a measure of the change of size of a sample as a function of temperature) and was shown to be more reliable [50]. Dynamic liquid–solid ratio experiments were then used to offer greater information regarding rehydration of foodstuffs [51] thanks to the low experimental time, allowing several non-destructive repeats over the course of the dehydration of a sample.

These experiments opened the door for CW-NMR methods to evaluate other dynamic processes, such as the oil content of corn kernels using commercial instruments such as the Varian model PA7 analyser with an integrator [52] or those involving fats in the food industry [46] and the effects of temperature on these processes [53]. This method also found application non-invasively evaluating the flowing process streams themselves [54] directly within the production line.

Several commercial instruments, such as the Newport Wide-Line Nuclear Magnetic Resonance Analyser or quantity Analyser, were also developed to facilitate industrial measurements for some of these applications and for other material samples, although their use was and is very limited.

The amplitude measurement that is most widely used is for an alternative design of magnetometer to that described previously, where instead of sweeping the frequency to find a resonance, a pre-polarised sample is detected remotely from the field in a traditional CW-NMR at fixed frequency [55]. The amplitude of the absorption signal in the remote CW-NMR is then inversely proportional to the field of interest. In the work of Woo, the setup is improved to allow for the measurements of magnetic fields as low as a few µT [56].

7. Advances in Electronics

From the late 1980s onwards CW-NMR became largely shelved, except for educational purposes and a few niche applications, as electronic advances made pulsed magnetic resonance the more powerful of the two techniques. A small group of researchers however continued to explore the potential of this technique. In this section we review a number of applications and modifications to the original technique, which in some way utilize electronics that were not available during the original development period.

7.1. Magnetometers

The sensitivity of a magnetometer is dependent on the range of fields which it is measuring and, as such, the smaller the sample and RF coil can be, the greater the sensitivity of the instrument. With a fully miniaturised sample and coil, it then becomes desirable to reduce the overall size of the electronics that drive the system. In 1998, Boero et al. [57] developed a CW-NMR device on a chip by electrodepositing a copper spiral coil onto glass next to a CMOS integrated bridge circuit (tuned with an MV209 Epicap Diode, On Semiconductor, Pheonix, USA), which undertakes signal amplification and detection, with an approximate overall size of 6 mm × 18 mm. The tuning of the device and frequency sweeping is computer controlled and the signal is digitized with a PC ADC (Analogue to Digital Converter).

One of the areas critical to CW-NMR that has seen the greatest development in recent decades is the generation of radio frequency. In the work of Wu et al. [58] for example, a digital RF generation system is used to provide energy to the sample and is also inductively coupled to a marginal oscillator (as described previously) which is used for detection. A Direct Digital Synthesiser (DDS) and Phased Locked Loop (PLL) are controlled by an 8051 microcontroller and generate a frequency sweep.

The previous work still utilises oscillator (and therefore analogue) signal detection. In the work of Begus and Fefer [59], attempts are made to replace as many analogue elements as possible with digital versions to improve stability and sensitivity. The system uses a similar front end to that in the original Rollin [12] paper, but with a temperature controlled DDS to supply the RF through a resistor to the tank circuit with a voltage tuned capacitor. This signal is then demodulated using the DDS as a reference before utilizing software lock-in detection on a Digital Signal Processor IC.

An alternative approach is seen in the work of Geršak et al. [60], which utilizes several benchtop instruments controlled by a PC running LabVIEW (National Instruments, Austin, TX, USA) to generate the necessary signals and collect the resulting spectra using a cross coil system as described previously.

7.2. Imaging

Another area that has benefitted greatly from advances in electronics is imaging. Most work in this area is based around the use of hybrid junctions, which are commercially available in various frequencies. The hybrid junction is a long-standing four-arm radio frequency and microwave component, designed such that a signal incident in any one arm is divided between two others, and not present on the fourth. This leads to interesting behavior if two coherent signals are incident on an arm each, as their sum will be present on the third arm and their difference on the fourth. Furthermore, if one of the arms is terminated with an appropriate impedance, one has incident RF and the third is connected to a circuit which absorbs the RF energy, the fourth arm will have an RF voltage proportional to the amount of energy that has been used. In this way, such a system can be seen as a type of bridge circuit if a tank circuit and terminator are connected to two branches, with an RF on a third. If there is an impedance mismatch between the terminator and a tank circuit (with the inductor containing the sample), the fourth branch outputs an RF voltage inversely proportional to the absorption. Such a circuit can be seen at the heart of a design by Lurie for imaging solids [61], followed by rectification with a diode detector. In the Lurie paper [61], and more recently in an extension of this work to image in three dimensions by Fagan [62], a small audio frequency modulation (1 kHz) is

superimposed in the magnetic field sweep voltage. The output of the diode detector is then fed to the input of a lock-in amplifier with the same 1 kHz signal used as a reference, thus almost eliminating the noise and amplifying only the NMR signal, a schematic for which is displayed in Figure 20. This is essential in the case of imaging as the already minimal signal is further minimized given the localization of magnetic moments of interest by the 3D gradient coils, which are also included.
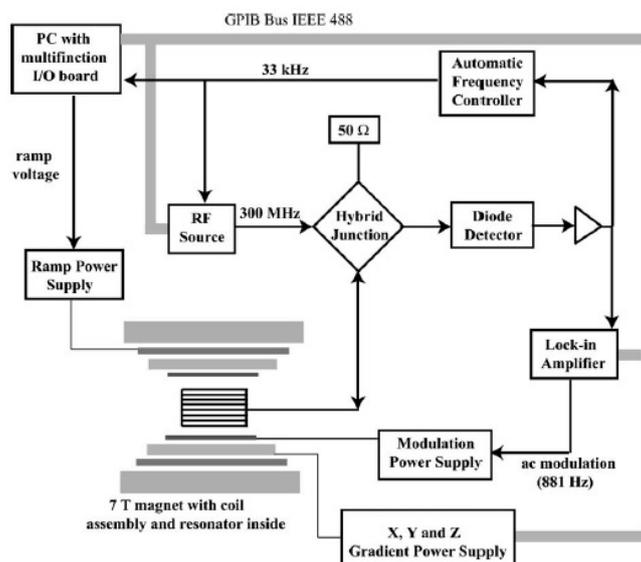
Figure 20. Block diagram of a setup for 3 dimensional continuous wave NMR imaging. (reproduced with permission from [62]. Copyright Elsevier, 2005).

7.3. Updated Measurements of Relaxation Parameters

We have recently presented an updated measurement method [63] based on the work of Look and Locker [43] utilizing direct signal capture and sweep signal generation with a National Instruments Data Acquisition card and PC to automatically acquire T_1 curves. A method was also proposed to eliminate the effect of the oscillator parameters on the resulting measurements by using end-point calibration.

8. Future Developments

One of the most ubiquitous building blocks for modern electronics is the microcontroller, which has become better and better equipped with peripherals as each year passes. The Teensy microcontroller [64] is an excellent example of this which, for less than USD25, has an ADC and DAC (Digital to Analogue Converter) which runs at 18 MHz. These are also easily extended with a plethora of extra modules that bring additional functionality. In Figure 21 we show typical data from a teaching CW-NMR system (LD Didactic GmbH, Hürth, Germany) with a sample of 20 cS PDMS oil and digitization of the signal resulting from the relaxation measurement described in [63]. The sweep coil rate is set at 10 Hz and the audio capture rate is set to 44.1 kHz, with 16 bit data saved to a raw file based on the example code provided at [65]. The Teensy and audio shield together cost approximately USD35, providing an exceptionally cost-effective data capture package, although alternatives are available such as the Raspberry PI [66] with a sound card. The ability to make an entire NMR based detection system for less than USD 200 will allow exploration of a wide array of new applications for which NMR was previously too expensive.
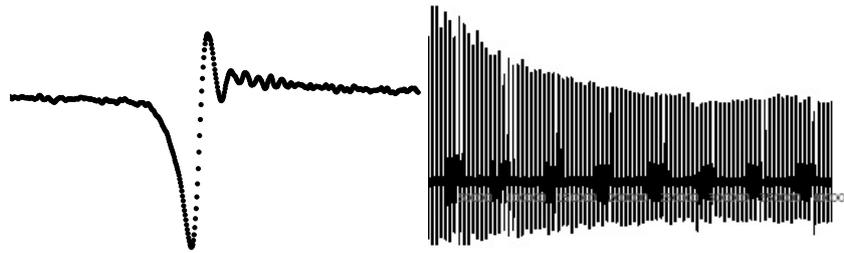
Figure 21. Example data to show how relaxation measurements can be obtained using low cost microcontroller capture.

Whilst using electromagnets gives flexibility in the choice of magnetic field and hence operating frequency, they also are bulky, expensive and consume significant power. Permanent magnets are less flexible and suffer from temperature drift but require no external power source and hence consume no power. Modern magnet technology, particularly that using Neodymium Iron Boron (NdFeB) magnets, do however provide small size, low-cost magnets in the field range that equates to a NMR frequency up to 20 MHz. There have been many reports over the years of how to achieve field uniformity from permanent magnets, including the use of pole pieces [67], or with current developments in 3D printing offering exciting potential for a simple route to custom design such magnets directly [68]. Similarly, magnet designs for pulsed NMR have become sufficiently homogeneous for achieving spectroscopy [69,70], which should also be sufficient for CW-NMR relaxation time measurements. In Figure 22, we show the electromagnets in a teaching CW-NMR system (LD Didactic GmbH, Hürth, Germany) replaced with a pair of low-cost NdFeB magnets with the NMR signal from water on the oscilloscope.
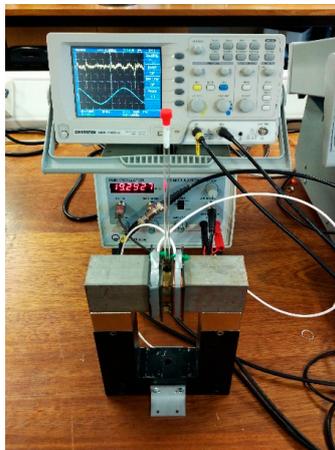
Figure 22. Electromagnets can be substituted for low-cost, modern NdFeB magnets.

9. Conclusions

In this article we have reviewed the electronics required to make measurements of various samples using continuous wave NMR. CW-NMR will never directly compete with pulsed NMR systems in providing a universal tool capable of measurements over a wide range of T_1, T_2* and T_2^{eff} or in measuring diffusion and over a range of magnetic fields. It does however provide an exciting opportunity for easily automated, low cost measurement applications. Although Pulsed NMR has been shown to be an effective analysis tool for the food and drinks industries (see for example recent reviews [71,72]), the limitations of cost, complexity and power consumption of pulsed techniques have to a large extent consigned these to the literature. We have shown however that where there is a targeted application for which the measurement range is clearly defined, CW-NMR may now

be capable of providing a cost effective industrial solution. Challenges still lie in the continued development of homogeneous magnets, perhaps with pole pieces displaying sufficient homogeneity or T_2^* measurements, however the range of electronics readily available, including low-cost DDS, microcontrollers, advanced amplification blocks, voltage controlled variable capacitors and hybrid junctions, does require a fresh look at Continuous Wave Nuclear Magnetic Resonance in a range of sectors.

References

1. Fox, M.; Rabi, I.I. On the Nuclear Moments of Lithium, Potassium, and Sodium. *Phys. Rev.* **1935**, *48*, 746–751. [CrossRef]
2. Breit, G.; Rabi, I.I. Measurement of Nuclear Spin. *Phys. Rev.* **1931**, *38*, 2082–2083. [CrossRef]
3. Purcell, E.M.; Torrey, H.C.; Pound, R.V. Resonance Absorption by Nuclear Magnetic Moments in a Solid. *Phys. Rev.* **1946**, *69*, 37–38. [CrossRef]
4. Bloch, F.; Hansen, W.W.; Packard, M. Nuclear Induction. *Phys. Rev.* **1946**, *70*, 460–474. [CrossRef]
5. Mansfield, P. Multi-planar image formation using NMR spin echoes. *J. Phys. C Solid State Phys.* **1977**, *10*, 55–58. [CrossRef]
6. Arnold, J.T.; Packard, M.E. Variations in Absolute Chemical Shift of Nuclear Induction Signals of Hydroxyl Groups of Methyl and Ethyl Alcohol. *J. Chem. Phys.* **1951**, *19*, 1608–1609. [CrossRef]
7. Carr, H.; Purcell, E. Effect of Diffusion on Free Precession in Nuclear Magnetic Resonance Experiments. *Phys. Rev.* **1954**, *94*, 630–638. [CrossRef]
8. Lauterbur, P.C. C13 Nuclear Magnetic Resonance Spectra. *J. Chem. Phys.* **1957**, *26*, 217–218. [CrossRef]
9. Damadian, R. Apparatus and method for detecting cancer in tissue. U.S. Patent 3,789,832, 5 February 1974.
10. Larmor, J. LXIII. On the theory of the magnetic influence on spectra; and on the radiation from moving ions. *Philos. Mag.* **1897**, *44*, 503–512. [CrossRef]
11. Bloch, F.; Hansen, W.W.; Packard, M. The Nuclear Induction Experiment. *Am. Phys. Soc.* **1946**, *70*, 474–485.
12. Rollin, B.V. Nuclear paramagnetism. *Rep. Prog. Phys.* **1949**, *12*, 22–23. [CrossRef]
13. Andrew, E.R. *Nuclear Magnetic Resonance*; Cambridge University Press: Cambridge, UK, 1955.
14. Anderson, H.L. Precise Measurement of the Gyromagnetic Ratio of He^3. *Phys. Rev.* **1949**, *76*, 1460–1470. [CrossRef]
15. Waring, C.E.; Spencer, R.H.; Custer, R.L. A Bridged Tee Detector for Nuclear Magnetic Resonance. *Rev. Sci. Instrum.* **1952**, *23*, 497–498. [CrossRef]
16. Tuttle, W.N. Bridged-T and Parallel-T Null Circuits for Measurements at Radio Frequencies. *Proc. Ire* **1940**, *28*, 23–29. [CrossRef]
17. Collins, R.L. Automatic Bridge Balance for Nuclear Spin Resonance Spectrometer. *Rev. Sci. Instrum.* **1957**, *28*, 502–503. [CrossRef]
18. Application Note #3—About Lock-In Amplifiers. Available online: http://www.thinksrs.com/downloads/PDFs/ApplicationNotes/AboutLIAs.pdf (accessed on 31 August 2017).
19. Bloembergen, N.; Purcell, M.E.; Pound, V.R. Relaxation Effects in Nuclear Magnetic Resonance Absorption. *Phys. Rev.* **1948**, *73*, 679–712. [CrossRef]
20. Lembo, R.R.; Kowalewski, V.J. Leakage balance system for crossed coil NMR probes. *J. Phys. E Sci. Instrum.* **1975**, *8*, 632–633. [CrossRef]
21. 111B: Advanced Experimentation Laboratory Notes—NMR—Nuclear Magnetic Resonance Physics. Available online: http://experimentationlab.berkeley.edu/sites/default/files/writeups/NMR.pdf (accessed on 31 August 2017).
22. Pound, R.V.; Knight, W.D. A Radiofrequency Spectrograph and Simple Magnetic-Field Meter. *Rev. Sci. Instrum.* **1950**, *21*, 219–225. [CrossRef]
23. Donnally, B.; Sanders, T.M. Simple Transistor Marginal Oscillator for Magnetic Resonance. *Rev. Sci. Instrum.* **1960**, *31*, 977–978. [CrossRef]

24. Willingham, F.P. Developing Improved Nuclear Magnetic Resonance Marginal Oscillator Spectrometers for Advanced Teaching Laboratories. Ph.D. Thesis, Georgia Military College, Milledgeville, GA, USA, 1988.

25. Robinson, F.N.H. Nuclear resonance absorption circuit. *J. Sci. Instrum.* **1959**, *36*, 481. [CrossRef]

26. Robinson, F.N.H. A high field nuclear magnetic resonance probe using transistors. *J. Sci. Instrum.* **1965**, *42*, 653. [CrossRef]

27. Faulkner, E.A.; Holman, A. An improved circuit for nuclear magnetic resonance detection. *J. Sci. Instrum.* **1967**, *44*, 391. [CrossRef]

28. Deschamps, P.; Vaissiére, J.; Sullivan, N.S. Integrated circuit Robinson oscillator for NMR detection. *Rev. Sci. Instrum.* **1977**, *48*, 664–668. [CrossRef]

29. Wilson, K.J.; Vallabhan, C.P.G. An improved MOSFET-based Robinson oscillator for NMR detection. *Meas. Sci. Technol.* **1990**, *1*, 458. [CrossRef]

30. Knoebel, H.W.; Hahn, E.L. A Transition Nuclear Magnetic Resonance Detector. *Rev. Sci. Instrum.* **1951**, *22*, 904–911. [CrossRef]

31. Herold, E.W. Negative Resistance and Devices for Obtaining It. *Proc. Inst. Radio Eng.* **1935**, *23*, 1201–1223. [CrossRef]

32. Blankenburg, F.J.; Knispel, R.R.; Schmidt, V.H. Sensitive Low Level Transistorized NMR Spectrometer Employing Frequency Modulation. *Rev. Sci. Instrum.* **1966**, *37*, 1020–1023. [CrossRef]

33. Robinson, F. A convenient nuclear resonance magnetometer. *J. Phys. E Sci. Instrum.* **1987**, *20*, 502–504. [CrossRef]

34. Weyand, K. An NMR marginal oscillator for measuring magnetic fields below 50 mT. *IEEE Trans. Instrum. Meas.* **1989**, *38*, 410–414. [CrossRef]

35. Metrolab PT2025 NMR Precision Teslameter. Available online: http://www.metrolab.com/products/pt2025/ (accessed on 31 August 2017).

36. Zweers, A.E. Methyl Group Rotation and Nuclear Relaxation at Low Temperatures. Ph.D. Thesis, University of Leiden, Leiden, The Netherlands, 1976.

37. Veenendaal, E.J.; Hulstman, R.; Brom, H.B. A frequency-modulated Q-meter for very low-temperature NMR experiments. *J. Phys. E Sci. Instrum.* **1983**, *16*, 649–653. [CrossRef]

38. Court, G.R.; Houlden, M.A.; Bültmann, S.; Crabb, D.G.; Day, D.B.; Prok, Y.A.; Penttila, S.I.; Keith, C.D. High precision measurement of the polarization in solid state polarized targets using NMR. *Nucl. Instrum. Methods Phys. Res.* **2004**, *527*, 253–263. [CrossRef]

39. Keller, D. Uncertainty minimization in NMR measurements of dynamic nuclear polarization of a proton target for nuclear physics experiments. *Nucl. Instrum. Methods Phys. Res.* **2013**, *728*, 133–144. [CrossRef]

40. Drain, L.E. A Direct Method of Measuring Nuclear Spin-Lattice Relaxation Times. *Proc. Phys. Soc.* **1949**, *62*, 301–306. [CrossRef]

41. Firth, L.D. Relaxation time measurement by continuous-wave NMR. *Eur. J. Phys.* **1982**, *3*, 10–13. [CrossRef]

42. Donnally, B.L.; Enrique, B.G. Some Experiments on Nuclear Magnetic Resonance. *Am. J. Phys.* **1963**, *31*, 779–784. [CrossRef]

43. Look, D.C.; Locker, D.R. Nuclear Spin-Lattice Relaxation Measurements by Tone-Burst Modulation. *Phys. Rev. Lett.* **1968**, *20*, 987–989. [CrossRef]

44. Gooden, J.S. Nuclear Resonance and Magnetic Field Changes of 1 in 106. *Nature* **1950**, *165*, 1014–1015. [CrossRef] [PubMed]

45. Jacobsohn, B.A.; Wangsness, R.K. Shapes of Nuclear Induction Signals. *Phys. Rev.* **1948**, *73*, 942–946. [CrossRef]

46. Gabillard, R. A steady state transient technique in nuclear resonance. *Phys. Rev.* **1952**, *85*, 694–695. [CrossRef]

47. Shaw, T.; Elsken, R. Moisture determination, determination of water by nuclear magnetic absorption in potato and apple tissue. *J. Agric. Food. Chem.* **1956**, *4*, 162–164. [CrossRef]

48. Ladner, W.; Stacey, A. Measurement of moisture in a moving coal feed. *Br. J. Appl. Phys.* **1962**, *13*, 136. [CrossRef]

49. Oref, I. Fat content and liquid-to-solid ratio of chocolate by wide line nuclear magnetic resonance. *J. Am. Oil Chem. Soc.* **1965**, *42*, 425–427. [CrossRef] [PubMed]

50. Pohle, W.; Taylor, J.; Gregory, R. A comparison of nuclear magnetic resonance and dilatometry for estimating solids content of fats and shortenings. *J. Am. Oil Chem. Soc.* **1965**, *42*, 1075–1078. [CrossRef] [PubMed]

51. Hall, G.; Lawrence, J.; Simpson, R. Nuclear Magnetic Resonance as a Method for Continuously Monitoring Rehydration. *Nature* **1967**, *216*, 474–475. [CrossRef]

52. Conway, T. A wide line NMR RF saturation method to measure fat in moist samples of defatted corn germ. *J. Am. Oil Chem. Soc.* **1971**, *48*, 54–58. [CrossRef]

53. Mertens, W. The influence of temperature treatment on solid-liquid ratios of fats determined by wide-line NMR. *Can. Inst. Food Sci. Technol. J.* **1972**, *5*, 77–81. [CrossRef]

54. Rollwitz, W.L.; Persyn, G.A. On-stream NMR measurements and control. *J. Am. Oil Chem. Soc.* **1971**, *48*, 59–66. [CrossRef]

55. Pendlebury, J.; Smith, K.; Unsworth, P.; Greene, G.; Mampe, W. Precision field averaging NMR magnetometer for low and high fields, using flowing water. *Rev. Sci. Instrum.* **1979**, *50*, 535–540. [CrossRef] [PubMed]

56. Woo, B.; Kim, C.; Park, P.G.; Kim, C.; Shifrin, V. Low magnetic field measurement by a separated NMR detector using flowing water. *IEEE Trans. Magn.* **1997**, *33*, 4345–4348. [CrossRef]

57. Boero, G.; de Raad Iseli, C.; Besse, P.; Popovic, R. An NMR magnetometer with planar microcoils and integrated electronics for signal detection and amplification. *Sens. Actuators A Phys.* **1998**, *67*, 18–23. [CrossRef]

58. Wu, C.; Lv, F.; Chen, Y. A new control method to generate RF signal for a novel NMR magnetometer. In Proceedings of the Control and Decision Conference, Taiyuan, China, 23–25 May 2012; pp. 2773–2776.

59. Begus, S.; Fefer, D. DDS Based NMR Magnetometer in Slovenian Calibration Laboratory. In Proceedings of the Precision Electromagnetic Measurements Digest, London, UK, 27 June–2 July 2004; pp. 392–393.

60. Geršak, G.; Humar, J.; Fefer, D. Virtual instrument—The NMR magnetometer. In Proceedings of the Book of Summaries, XVII IMEKO World Congress, Dubrovnik, Croatia, 22–27 June 2003.

61. Lurie, D.J.; Mccallum, S.J.; Hutchison, J.M.S.; Aleccit, M. Continuous-wave NMR imaging of solids. *Magn. Reson. Mater. Phys. Biol. Med.* **1996**, *4*, 77–81. [CrossRef]

62. Fagan, A.J.; Davies, G.R.; Hutchison, J.M.S.; Glasser, F.P.; Lurie, D.J. Development of a 3-D, multi-nuclear continuous wave NMR imaging system. *J. Magn. Reson.* **2005**, *176*, 140–150. [CrossRef] [PubMed]

63. Morris, R.H.; Mostafa, N.; Parslow, S.; Newton, M.I. Transient effect determination of spin–lattice (TEDSpiL) relaxation times using continuous wave NMR. *Magn. Reson. Chem.* **2017**, *55*, 853–855. [CrossRef] [PubMed]

64. Teensy USB Development Board—PJRC Electronics Projects. Available online: https://www.pjrc.com/teensy/ (accessed on 31 August 2017).

65. Audio Recorder Example—Paul Stoffregen. Available online: https://github.com/PaulStoffregen/Audio/blob/master/examples/Recorder/Recorder.ino (accessed on 31 August 2017).

66. Raspberry PIRaspberry PI Foundation. Available online: https://www.pjrc.com/teensy/ (accessed on 31 August 2017).

67. Andrew, E.; Rushworth, F. Ring shims for coned magnet polecaps. *Proc. Phys. Soc. Sect. B* **1952**, *65*, 801–805. [CrossRef]

68. Huber, C.; Abert, C.; Bruckner, F.; Groenefeld, M.; Muthsam, O.; Schuschnigg, S.; Sirak, K.; Thanhoffer, R.; Teliban, I.; Vogler, C. 3D print of polymer bonded rare-earth magnets, and 3D magnetic field scanning with an end-user 3D printer. *Appl. Phys. Lett.* **2016**, *109*, 461–465. [CrossRef]

69. Jachmann, R.C.; Trease, D.R.; Bouchard, L.; Sakellariou, D.; Martin, R.W.; Schlueter, R.D.; Budinger, T.F.; Pines, A. Multipole shimming of permanent magnets using harmonic corrector rings. *Rev. Sci. Instrum.* **2007**, *78*, 035115. [CrossRef] [PubMed]

70. Danieli, E.; Mauler, J.; Perlo, J.; Blümich, B.; Casanova, F. Mobile sensor for high resolution NMR spectroscopy and imaging. *J. Magn. Reson.* **2009**, *198*, 80–87. [CrossRef] [PubMed]

71. Guthausen, G. Analysis of food and emulsions. *TrAC Trends Anal. Chem.* **2016**, *83*, 103–106. [CrossRef]

72. Dalitz, F.; Cudaj, M.; Maiwald, M.; Guthausen, G. Process and reaction monitoring by low-field NMR spectroscopy. *Prog. Nuclear Magn. Reson. Spectrosc.* **2012**, *60*, 52–70. [CrossRef] [PubMed]